

# Mass Distribution and Accretion of Sub-halos

Yun Li<sup>1\*</sup>, H.J. Mo<sup>1</sup>

<sup>1</sup>*Department of Astronomy, University of Massachusetts, Amherst, MA 01003, USA*

## ABSTRACT

We use the “Millennium Simulation” to study the mass function of accreted sub-halos during merger events in the dark halo assembly history. Our study includes three kinds of sub-halo mergers: (1) mergers that happen to the main progenitor of dark halos; (2) mergers that happen on the entire merging history tree of dark halos; and (3) mergers that leave *identifiable* sub-halos in present-day dark halos. We estimate the *unevolved* sub-halo mass functions (USMFs), for which sub-halo masses are measured at the times of their accretion. For sub-halos that merge into the main branch of a present-day dark halo, their USMF can be well described by a universal functional form, in excellent agreement with previous results. The same conclusion can also be reached for the USMF of all progenitors that have merged to become sub-halos during the entire halo merging history. In both cases, the USMFs are also independent of the redshift of host halos. Due to tidal disruption, only a small fraction of the accreted halos survive as sub-halos identifiable in the present-day dark halos. In cluster-sized halos, about 30% of the survived sub-halos are sub-subhalos, and this fraction decreases with decreasing halo mass. For given halo and sub-halo masses, the accretion time has very broad distribution, but the survived sub-halos are all accreted quite recently.

**Key words:** cosmology: theory — galaxies: formation — galaxies: halos — dark matter.

## 1 INTRODUCTION

In the past two decades, the Cold Dark Matter (CDM) model of structure formation has been widely adopted and serves well as a framework for modeling the galaxy formation. The understanding of CDM halo formation is a key factor to understand the formation process and properties of large-scale structure as well as the galaxies that form and evolve within the dark halos. There are multiple important properties regarding dark halo formation that have been intensively studied, including halo mass function (e.g. Bond et al. 1991; Lacey & Cole 1993; Sheth & Torman 1999), density profile (e.g. Navarro, Frenk & White 1997; Bullock et al. 2001b; Lu et al. 2006), angular momentum property (e.g. Barnes & Efstathiou 1987; Cole & Lacey 1996; Bullock et al. 2001a), mass accretion history (e.g. Zhao et al. 2003; Wechsler et al. 2002; Li et al. 2007), and clustering property (e.g. Mo & White 1996; Lemson & Kauffmann 1999; Sheth & Torman 1999; Sheth, Mo & Torman 2001; Gao et al. 2005).

Besides the properties mentioned above, halo-halo mergers and the subsequent evolution of resultant sub-halos have been of great interests recently, in both analytical models and  $N$ -body simulations (Sheth 2003; Gao et al.

2004; De Lucia et al. 2004; van den Bosch et al. 2005; Giocoli et al. 2008a,b; Angulo et al. 2008; Wetzell et al. 2008). Since galaxies are believed to initially reside at the center of and merge along with dark halos, these events are therefore highly correlated with galaxy evolution. In this scenario, mergers play a transitional role in converting central galaxies into satellite galaxies in the post-merger halos. They may also trigger the evolution of various galactic properties, such as the morphology, luminosity, color and spacial distribution (Barnes & Hernquist 1996; Naab & Burkert 2003; Hopkins et al. 2006; Maller et al. 2006; De Lucia & Blaizot 2007; McIntosh et al. 2008).

Although, from a phenomenological point of view, some observational statistics based on current sub-halo mass model matches well with the observations (Mandelbaum et al. 2006; Kim et al. 2008), our understanding of galaxy formation still needs improvements due to the insufficient modeling of various physical processes, such as cooling, feedback, and merging history. It is also ambiguous how exactly post-merger galaxies are linked with pre-merger dark halos, because once a merger happens, the subsequent tidal forces and dynamical friction will cause the sub-halo, formerly a host halo, to loose mass and possibly become completely destroyed. This process gives rise to several possible fates of the stellar components of the galaxies that merge along with the sub-halos (Yang et al. 2009).

\* E-mail: liyun@astro.umass.edu

Despite the details of how a satellite galaxy evolves in a denser environment, it is always important to quantify the mass function of the associated sub-halos at the time of merging, for several reasons. First, previous studies have suggested that mass is a key factor of various properties of dark halos, such as density profile (Navarro, Frenk & White 1997), sub-halo population (Gao et al. 2004), clustering property (Mo & White 1996). Secondly, and more importantly perhaps, different approaches such as the halo occupation distribution (HOD) or similar models (e.g. Berlind & Weinberg 2002; Zheng et al. 2005; Tinker et al. 2005; Wang et al. 2006) and conditional luminosity function (CLF) model (Yang et al. 2003; van den Bosch 2007), which base their galaxy statistics on host halo mass, have resulted in reliable descriptions of the distribution of galaxies. Therefore, to better understand the link between sub-halo mergers and post-merger galaxies, some important issues need to be addressed. For example, based on extended Press-Schechter formalism and direct  $N$ -body simulations, van den Bosch et al. (2005) and Giocoli et al. (2008a) found that the unevolved sub-halo mass function (USMF) of the progenitors that merged into halo main branch follows a universal form. Their findings are useful because the results can be linked to the number of central galaxies that may have turned into satellite galaxies through *direct* merger into a final halo. However, this information is insufficient to account for *all* incidences of mergers during the entire galaxy assembly history, because the hierarchical nature of CDM model suggests that sub-halos were independent host halos before the time of accretion, and it is likely they inherit the generic sub-halo population by the time when they became sub-halos. Thus, to investigate the possible effects on the statistics of galaxy properties from the angle of sub-halos, one needs to further clarify two questions. First, is the USMF really generic (i.e., does it depend on other quantities such as redshift than halo mass)? Second, what may be the difference if one takes into account the inherited sub-halo statistics of a sub-halo itself? Today, high resolution  $N$ -body simulations provide a direct way to measure the merger statistics of dark halos to relatively high redshift with a good mass resolution.

In this paper, we take advantage of a large  $N$ -body simulation and its distinguished sub-halo statistics to answer the questions mentioned above. This paper is organized as follows. In section 2 we give a brief overview of the simulation and the algorithm used to construct the halo merging tree. In section 3 we describe in detail how to use the merging tree to identify halo-halo mergers during the halo accretion history, and further derive the unevolved mass function of the sub-halos characterized in several different ways. In section 4 we study the accretion time of sub-halos and mass function of sub-halos accreted at given redshift. Lastly in section 5 we summarize our results.

## 2 THE SIMULATION

In this paper we use the “Millennium Simulation” (MS) carried out by the Virgo Consortium (Springel et al. 2005). We have used the same simulation data in an earlier paper to study the age dependence of dark halo spacial distribution (Li et al. 2008). This simulation follows the evo-

lution of  $2160^3$  dark matter particles in a cubic box of  $500 h^{-1}\text{Mpc}$  on a side, with a mass resolution of approximately  $8.6 \times 10^8 h^{-1}\text{M}_\odot$  per particle. The simulation adopts a flat  $\Lambda\text{CDM}$  model with  $\Omega_{\text{M}} = \Omega_{\text{dm}} + \Omega_{\text{b}} = 0.205 + 0.045 = 0.25$ , where  $\Omega_{\text{dm}}$  and  $\Omega_{\text{b}}$  stand for the current densities of dark matter and baryons respectively; the linear r.m.s. density fluctuation in a sphere of an  $8 h^{-1}\text{Mpc}$  radius,  $\sigma_8$ , equals 0.9; and the dimensionless Hubble expansion parameter  $h = 0.73$ . There are 63 snapshot outputs between  $z = 0$  and  $z = 80$ , with a roughly even placement in  $\ln(1+z)$  space. The standard Friends-Of-Friends (FOF) algorithm with a linking length parameter  $b_1 = 0.2$  is used to identify FOF dark halos. Only FOF halos with more than 20 particles are resolved. Based on the FOF catalogue, each FOF halo is then assigned a corresponding “virial mass”,  $M_{\text{h}}$ , so that the average density contrast between the “virial halo” and cosmic critical density  $\rho_{\text{c}}$  is approximately 200. The value of  $M_{\text{h}}$  is slightly smaller (about 5 – 10% on average) than the total mass of the corresponding FOF halo, and in general  $M_{\text{h}}$  accounts for the mass in the central part. This definition is therefore less affected by the so-called linking-bridge problem that can cause uncertainties in the halo mass. In what follows, we always use “virial mass”,  $M_{\text{h}}$ , as the halo mass. In order to ensure robustness and completeness of our sub-halo analysis, we only use sub-halos with masses above a mass limit  $M_{\text{lim}} = 2 \times 10^{10} h^{-1}\text{M}_\odot$ . This mass limit is slightly higher than the re-simulated halos used by Giocoli et al. (2008a), but the simulation volume of the MS allows us to use many more halos to gain better statistics.

The halo merging trees in the MS are constructed on the basis of sub-halos. In each FOF group, self-bound sub-structures (sub-halos) are further identified using SUBFIND (Springel et al. 2001), with the largest “sub-halo” being the “main” halo. A sub-halo 1 at redshift  $z_1$  is considered a progenitor of another sub-halo 2 at  $z_2$  ( $z_1 > z_2$ ) if the majority of its most bound particles are in sub-halo 2. In the literature, merging history trees based directly on FOF halos are widely employed to study the mass accretion history of dark halos. The “sub-halo”-based linking algorithm used in the MS, however, has special advantages over the FOF merging tree in the study of the evolution of sub-halos. By definition, this algorithm enables a more clear-cut history tracer of sub-halos (see e.g., Fakhouri & Ma 2008).

## 3 UNEVOLVED SUB-HALO MASS FUNCTIONS

Mergers are important events during the lifetime of a galaxy. If there exists a one-to-one correspondence between a central galaxy and a host halo, then all galaxies are initially central galaxies at some high redshift in the hierarchical scenario of structure formation. Subsequent halo mergers play an crucial role in galaxy evolution, in the sense that a central galaxy will be formally transferred into a satellite galaxy and perhaps evolve passively afterwards without a significant amount of star formation. As mentioned before, galaxy properties may be highly correlated with their host halo mass. Understanding the mass function of the progenitors of the sub-halos at the time of accretion is a key step in understanding the formation and evolution of satellite galaxies. In what follows we will refer the mass function of

sub-halos at accretion as the the unevolved sub-halo mass function (USMF), which reflects the fact that the sub-halos at the times of accretion have not yet been processed by dynamical effects, such as tidal stripping. In the rest of this section, we will discuss the USMF of sub-halos in the following three categories:

- (i) In Sub-section 3.1, we focus on sub-halos on the main branch of the merging tree, i.e., progenitors that directly merge with the main progenitors of dark halos. The same case has been studied by Giocoli et al. (2008a).
- (ii) In Sub-section 3.2, we include all sub-halos that have merged into the entire merging tree of a dark halo.
- (iii) Finally in Sub-section 3.3, we focus on sub-halos that are directly identifiable in the present-day halos, the so-called “survived sub-halos”.

### 3.1 Main branch sub-halos

To construct the halo main branch, we start with the final halo at a given redshift  $z_h$  (in this paper,  $z_h = 0$  unless otherwise mentioned), and trace its most massive progenitor (the main progenitor) in the adjacent snapshot at higher redshift. We then repeat this procedure for the main progenitor till the progenitor mass is too small to be resolved. During this procedure, we also search the indices of all other progenitors that have directly merged into the main progenitor. If a progenitor was an independent halo before merger, we register its mass as well as the redshift at which it was accreted (the redshift information will be used later to study the mass function of sub-halos at given accretion time). This method eliminates cases where progenitors were already sub-halos of other more massive progenitors at the time of merging. With the information collected in this way, we are able to construct the USMF of main branch sub-halos. The results are plotted in Fig. 1 for host halos of different masses (as indicated).

We adopt the same functional form proposed by Giocoli et al. (2008a) to fit the simulation results. Given a final halo (host halo) mass  $M_h$  and a sub-halo mass *at accretion*,  $M_{acc}$ , the USMF,  $F$ , is written as

$$\begin{aligned} F\left(\frac{M_{acc}}{M_h}\right) &= \frac{dN}{d\ln(M_{acc}/M_h)} \\ &= a \left(\frac{M_{acc}}{M_h}\right)^b \exp\left[-c \left(\frac{M_{acc}}{M_h}\right)^d\right], \end{aligned} \quad (1)$$

where  $N$  stands for the number of sub-halos that were accreted and  $a, b, c, d$  are fitting parameters. At the low-mass end ( $M_{acc}/M_h \rightarrow 0$ ), this is a power-law, while at high-mass end ( $M_{acc}/M_h \rightarrow 1$ ), the function decreases exponentially with  $(M_{acc}/M_h)^d$ . If the other parameters are fixed,  $a$  represents the overall amplitude,  $b$  indicates the low-mass end power-index,  $c$  indicates the transitional point where the curve changes its shape, and  $d$  determines the steepness of the exponential decline. However, different combinations of parameters can result in  $F$  with similar shapes within the mass range probed here ( $\log_{10}[M_{acc}/M_h] \in [-4, 0]$ ). Therefore we do not intend to fit the result for each host-halo mass bin separately. Instead, we use all the mass bins to obtain an overall fit, which is shown as the solid line in the last panel. For comparison the best-fit USMF obtained

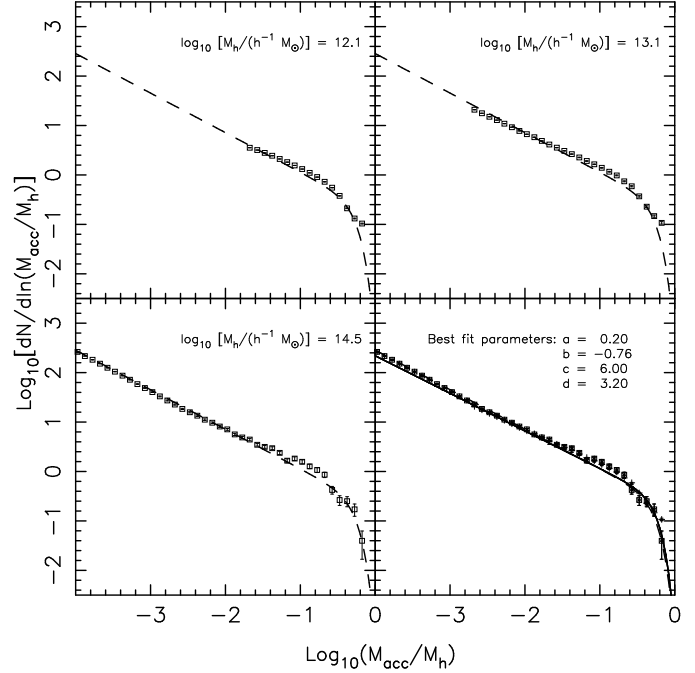


**Figure 1.** The USMF of main branch sub-halos. The *upper two panels and the lower left panel* show the USMF of  $z_h = 0$  halos with  $M_h = 10^{12.1}, 10^{13.1}, 10^{14.5} h^{-1} M_\odot$ , respectively. Data points are the average over all halos with mass  $M_h$ , error bars represent the standard error of the average. For reference, in each panel we also plot, with identical dashed lines, the best-fit USMF from Giocoli et al. (2008a). In the *lower right panel*, we summarize all the data from previous panels, and plot equation (1) (in thick solid line) with an empirical set of parameters (as indicated in the panel) which provides a universal fit to all of our data.

from Giocoli et al. (2008a) is shown in each panel of Fig. 1 as the dashed curve.

Our results show an overall excellent agreement with the result by Giocoli et al. (2008a). The values of the fitting parameters we obtain are very close to what were proposed by Giocoli et al. (2008a), with only slight difference. For instance, we find the low-mass end power-law index  $b = -0.76$ , which is a slightly shallower than their  $-0.8$ . Our slope is chosen so as to reconcile the slightly higher “shoulder” found in the mass range  $\log_{10}(M_{acc}/M_h) \in [-1.5, -0.5]$ . Note that for halos with  $M_h = 10^{12.1} h^{-1} M_\odot$ , we do not have data points that cover far enough into the power-law part.

We also estimate the USMF for host halos identified at redshift  $z_h = 1$ , and the result is shown in Fig. 2. Although the cosmic density field has evolved significantly during the time interval from  $z_h = 1$  to  $z_h = 0$ , the USMF at  $z_h = 1$  has the same form as that for  $z_h = 0$  halos. All these suggest that the USMF of the main branch sub-halos has a universal form, independent of host halo mass and the redshift at which the host halo is identified.

### 3.2 All sub-halos on the merging tree

The merging history of a dark halo is in general quite complex. At lower redshifts, after a halo has assembled its main body, mergers may primarily happen on the main branch. However, at higher redshift, when a large fraction of the

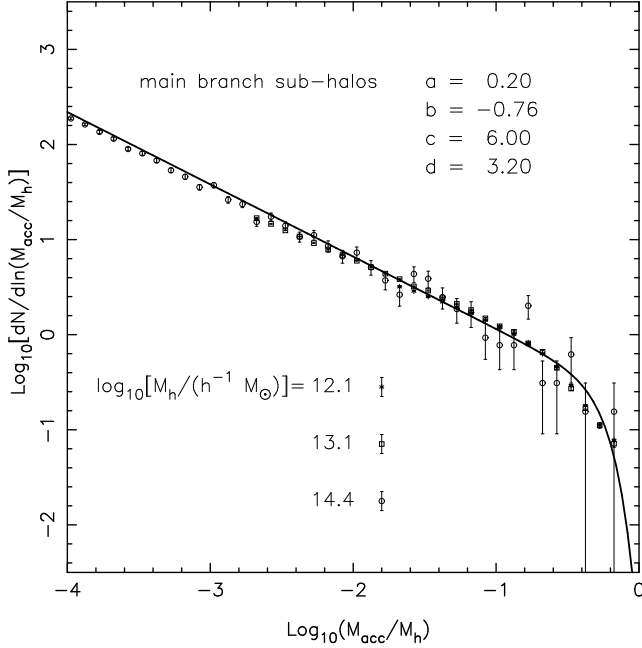


**Figure 2.** The USMFs of main branch sub-halos for host halos at  $z_h = 1$ . Different symbols represent the data points for host halos with different masses (as indicated), and the solid line is the universal fits we have obtained from  $z_h = 0$  halos.

final halo mass was still part of smaller progenitors, mergers that take place on the sub-branches of the merging tree can no longer be neglected. In addition, the sub-halos that merge into the sub-branches may still present at the time when their host halos merge into larger halos. Although it is likely that most sub-halos that merge at high redshift may have already been dissolved by dynamical friction and tidal stripping by the time when the final halo assembles, the satellite galaxies that merged along with them may be more resistant to these dynamical effects. Therefore, it is interesting to investigate the statistical properties of these merging events.

In order to quantify the USMF of all sub-halos in the entire merging tree of a halo, we start from the final host halo and trace back to all its progenitors that have ever merged as a sub-halo, regardless whether the merger takes place on the main branch or sub-branches. Once we found a merger between two independent halos, we register the mass of the sub-halo and the time of merger.

Fig. 3 shows the USMF of all sub-halos in the halo merging tree, in the same way as Fig. 1 for sub-halos in the main branch. Interestingly, equation (1) still provides a good description of the USMF in this case, although the fitting parameters are different from those for the sub-halos in the main branch (see the solid line in the lower right panel and the values of the fitting parameters listed in the panel). Comparing the results here with those shown in Fig. 1, we see that the overall amplitude here is higher, due to the fact that sub-halos on sub-branches are also included. In addition, the increase in the amplitude is much larger for low-mass sub-halos than for massive ones, giving rise to a steeper power-law slope in the low-mass end – compare the data points

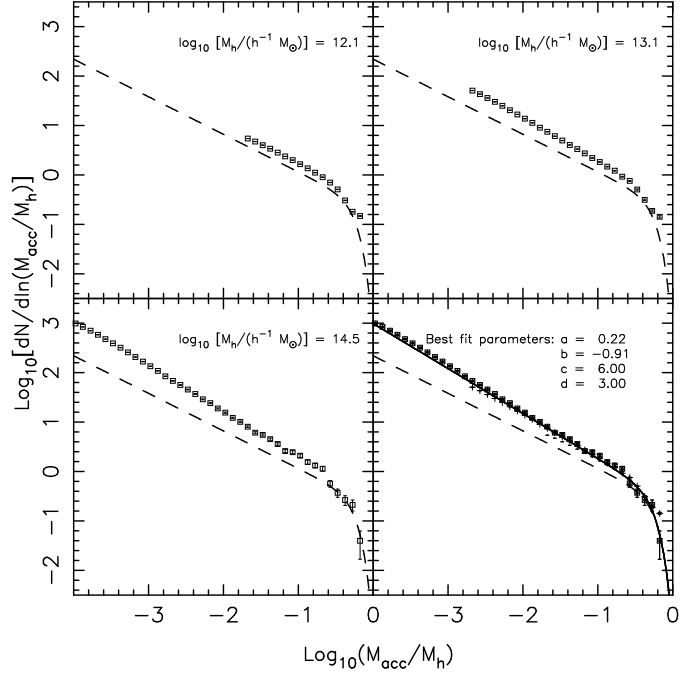


**Figure 3.** The USMF of all sub-halos that merged on the entire halo merging tree, plotted in the same way as in Fig. 1. Here, for reference purpose, the dashed lines in each panel represent our “universal” fit of the USMF of the main branch sub-halos (the same as the thick solid line in the lower right panel of Fig. 1). Similar to Fig. 1, in the *lower right panel* we choose an empirical set of parameters (values as indicated in the panel) for equation (1) and plot in thick solid line, so that it simultaneously fits all data points from the previous three panels.

in each panel with the dashed curve that shows the fitting result of the USMF for sub-halos in the main branch. This is not difficult to understand. When we trace back in time to all branches on the merging tree, the number of sub-branches on the halo merging tree increases significantly with redshift due to bifurcation. Meanwhile, the average mass of progenitors drops dramatically because of mass conservation. Since our mass function is based on the unevaluated merger progenitors, more mergers of low-mass sub-halos are expected at higher redshift.

In Fig. 4 we show the USMF of all sub-halos for host halos identified at  $z_h = 1$ . Clearly, this USMF shows remarkable agreement with that for  $z_h = 0$  host halos, indicating that the USMF of sub-halos in the entire merging tree also has a universal form.

Let  $F_{\text{Tree}}$  and  $F_{\text{MB}}$  represent our universal fits to the USMFs of all sub-halos and the main branch sub-halos, respectively. Fig. 5 shows the ratio of these two functions as a function of  $M_{\text{acc}}/M_h$ . At the low-mass end  $F_{\text{Tree}}$  is about four times  $F_{\text{MB}}$ , while at the high-mass end they are nearly equal. The significant excessive rate of mergers at low-mass end seen in the ratio indicates the abundance of sub-halos that were accreted by the sub-branches of the merging tree (we will discuss in details later). These sub-halos may end up as the so-called sub-subhalos when they finally settle in the main progenitor (Yang et al. 2009).

As we have seen, the USMF of the main branch sub-halos is universal, independent of the mass and redshift of

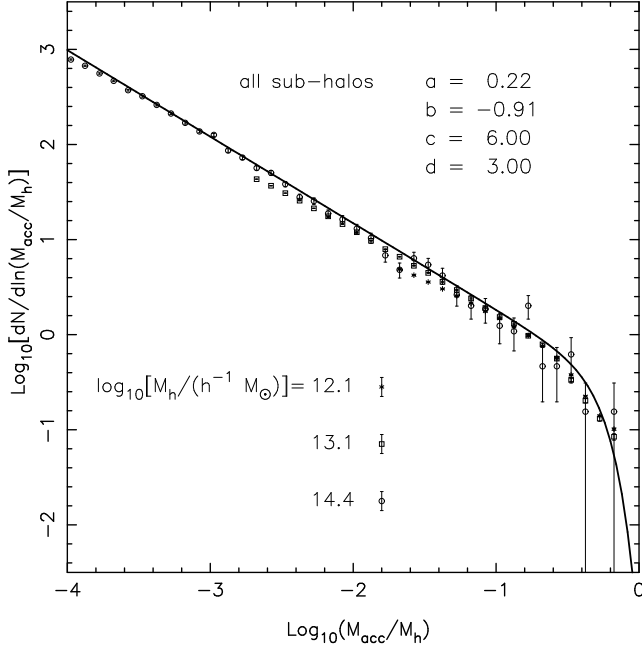


**Figure 4.** The USMFs of all sub-halos for host halos at  $z_h = 1$ . Same as in Fig. 2, different symbols represent the data points for host halos with different masses (as indicated), and the solid line is the universal fit we have obtained from  $z_h = 0$  halos.

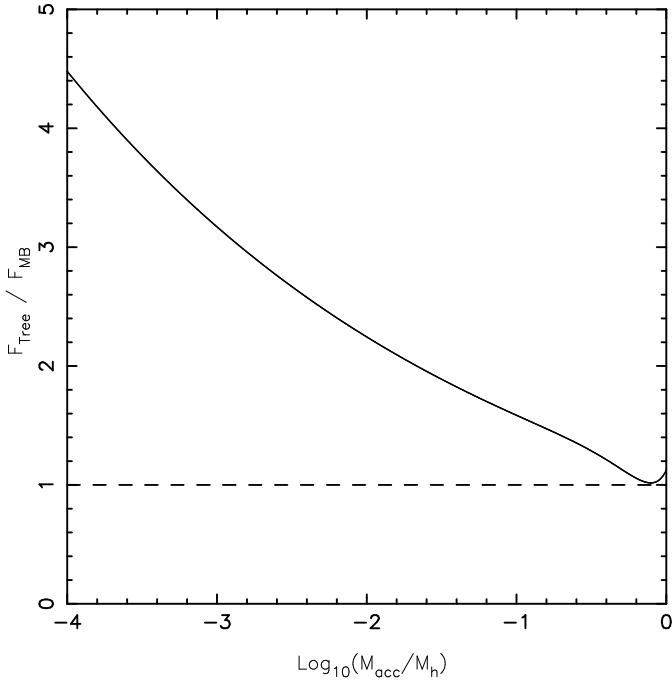


**Figure 5.** The solid line shows the USMF of all sub-halos divided by the USMF of main branch sub-halos, based on the two fitting results we have obtained. Dashed line is a reference line of  $y = 1$ .

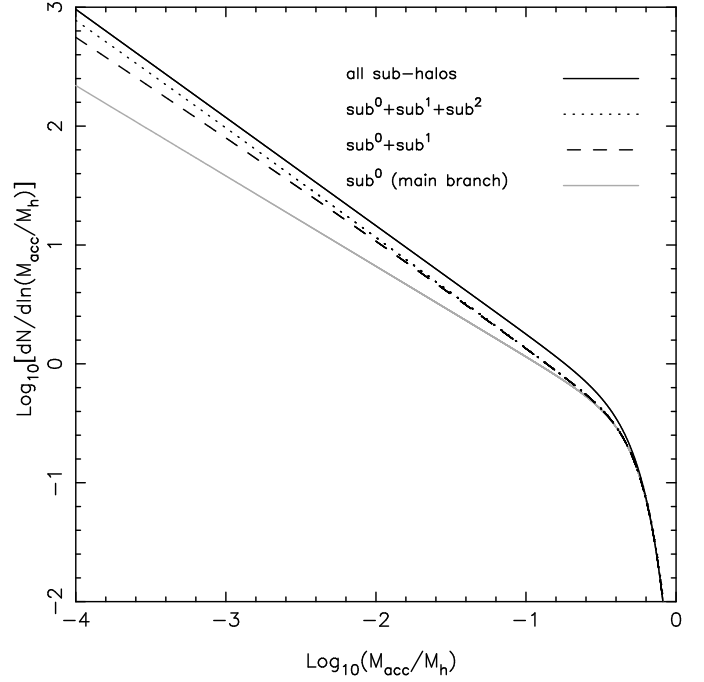


**Figure 6.** Comparison between the USMF of main branch sub-halos (gray solid line, which is same as the solid line in the lower right panel of Fig. 1), all sub-halos (dark solid line, the same as the solid line in the lower right panel of Fig. 3), the sum of  $\text{sub}^0$  and  $\text{sub}^1$ -halos (dashed line), as well as the sum of  $\text{sub}^0$ ,  $\text{sub}^1$  and  $\text{sub}^2$ -halos (short-dashed line) from the model prediction (equation [3]).

host halos. This proposition has been adopted by some authors when modeling the population of satellite galaxies in dark matter halos (e.g. Yang et al. 2009). Yang et al. (2009) assumed that the USMF of main branch sub-halos is self-similar, and sub-halos can be divided into different “levels”. Since sub-halos can themselves be considered as host halos at the time of accretion, their sub-halos (referred to sub-sub-halos, or  $\text{sub}^1$ -halos) are also expected to obey the universal USMF. Similarly, all levels of sub-halos ( $\text{sub}^i$ -halos,  $i = 0, 1, 2, 3, \dots$ , where superscript ‘0’ stands for the main branch sub-halos) should have the same form of USMF. The summation of the USMFs at all levels should be equal to the USMF of sub-halos in the whole tree. To test this, we rewrite equation (1) as

$$\begin{aligned} n_{\text{un},0}(M_{\text{acc}}|M_h) &= \frac{dN}{dM_{\text{acc}}} \\ &= \frac{a}{M_h} \left( \frac{M_{\text{acc}}}{M_h} \right)^{b-1} \exp \left[ -c \left( \frac{M_{\text{acc}}}{M_h} \right)^d \right]. \end{aligned} \quad (2)$$

Since equation (2) is universal, it should apply to all  $\text{sub}^i$ -halos ( $i = 0, 1, 2, 3, \dots$ ). This allows us to calculate the conditional USMF of  $\text{sub}^i$ -halos given the host halo mass  $M_h$ ,

$$\begin{aligned} n_{\text{un},i}(M_{\text{acc},i}|M_h) &= \\ &= \int_0^{M_h} n_{\text{un},0}(M_{\text{acc},i}|M_{\text{acc}}) n_{\text{un},i-1}(M_{\text{acc}}|M_h) dM_{\text{acc}}. \end{aligned} \quad (3)$$

Fig. 6 shows the comparison between the USMF of main branch sub-halos, all sub-halos, the sum of  $\text{sub}^0$  and  $\text{sub}^1$ -

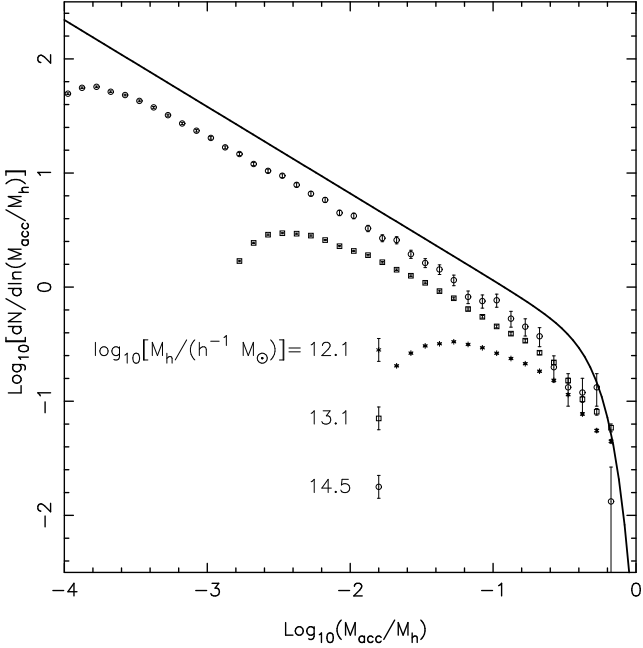


**Figure 7.** The “unevolved” mass function of sub<sup>A</sup>-halos,  $F'_{\text{sub}^A}$ . Different symbols represent different final host halo mass. The thick solid line is the universal form of the USMF of main branch sub-halos,  $F_{\text{MB}}$ .

halos, as well as the sum of sub<sup>0</sup>, sub<sup>1</sup> and sub<sup>2</sup> -halos predicted by equation (3). The best-fit parameters used in the calculation are indicated in the lower-right panels of Figs. 1 and 3, respectively. Clearly, as we include more levels of sub-halos, the summation of their USMF approaches asymptotically to that of all sub-halos. It is also interesting that sub<sup>1</sup>-halos contribute the largest fraction of small sub-halos that are not included in the USMF of the main branch sub-halos. Note that in the mass range  $M_{\text{acc}}/M_h \in [-2, -0.3]$ , the difference between the dark solid line and the short-dashed line in Fig. 6 is more significant. It is unclear if this difference is real, or it is due to the limited statistics of the simulation data.

### 3.3 Survived sub-halos

In the two cases discussed above, the USMFs do not seem to depend on the final halo mass or redshift, and appear to be “universal”. However, once a sub-halo merges into a host halo, it will undergo a number of non-linear processes such as dynamical friction, which causes the sub-halo to merge into the center of the host, and tidal stripping, which causes it to lose mass or to be completely destroyed. Therefore, the number of *survived* sub-halos may be significantly lower than the sub-halo abundance described by the USMF. Note that there are two kinds of survived sub-halos: those that directly merged into the main branch, and those that were already a sub-halo of a larger progenitor when being accreted by the main progenitor. Throughout this paper, we refer to the former as sub<sup>A</sup>-halos, and the latter as sub<sup>B</sup>-halos, which are also known as sub-subhalos.

After removing the sub<sup>B</sup>-halos from our survived sub-halo catalogue, we construct the “unevolved” mass function of the sub<sup>A</sup>-halos. The quotation marks are used to

indicate that a certain fraction of the main branch sub-halos have been completely destroyed, although the sub-halo mass used here is the mass at the time of accretion,  $M_{\text{acc}}$ . Since the destroyed sub-halos are not included, we use  $F'_{\text{sub}^A}$  to distinguish this “unevolved” sub-halo mass function from the USMF discussed previously. Fig. 7 shows the “unevolved” sub-halo mass function so defined for host halos with  $M_h = 10^{12.1}, 10^{13.1}$ , and  $10^{14.5} h^{-1} M_\odot$ , respectively. Apparently the shape of  $F'_{\text{sub}^A}$  depends strongly on host halo mass. Unlike the USMFs discussed previously, for given host halo mass  $M_h$ ,  $F'_{\text{sub}^A}$  is not a monotonic decreasing function of sub-halo mass, but rather, its amplitude lowers when the sub-halo mass becomes very small. This is caused by the dynamical processes after the accretion of sub-halo. Note, however, that the value of  $M_{\text{acc}}/M_h$  at which  $F'_{\text{sub}^A}$  peaks depends on the mass limit  $M_{\text{lim}}$  adopted. There is a high probability that a sub-halo initially accreted with mass  $M_{\text{acc}}$  slightly above  $M_{\text{lim}}$  to become smaller than  $M_{\text{lim}}$  during the post-accretion phase and thus to be marked as “destroyed”. In addition, smaller sub-halos are more difficult to survive, because on average they were accreted into their hosts earlier.

Fig. 7 may be used to estimate the number fraction of sub-halos that survive the mass-loss process. For example, for halos with  $M_h \sim 10^{14.5} h^{-1} M_\odot$ , about 62% of the accreted main branch sub-halos above the mass limit  $M_{\text{lim}}$  have been completely destroyed, this fraction increases to  $\sim 78\%$  and  $\sim 84\%$  for  $M_h = 10^{13} h^{-1} M_\odot$  and  $M_h = 10^{12} h^{-1} M_\odot$  halos, respectively. This trend may be understood since small systems start to accrete progenitors earlier, and so their main branch sub-halos are subject to mass loss and destruction for a longer time. The shape of  $F'_{\text{sub}^A}$  for host halos at  $z_h = 1$  is similar to that at  $z_h = 0$ . However, the similarity here is less meaningful, because the shape of  $F'$  is highly affected by the non-linear effects during sub-halo mergers, which is a very stochastic process (Angulo et al. 2008).

The result presented here is consistent with that of Giocoli et al. (2008a, their Fig. 4), although their result is based on the *evolved* sub-halo mass function. They found that for small host halos, there are less sub-halos with the same fractional mass,  $M_{\text{sub}}/M_h$  (where  $M_{\text{sub}}$  is the *current* mass of survived sub-halos), than more massive host halos. In Fig. 7, we have showed that for smaller host halo mass, the amplitude of the “unevolved” sub<sup>A</sup>-halo mass function,  $F'_{\text{sub}^A}$ , is also lower. In addition, according to Giocoli et al. (2008a, and reference therein), for evolved sub-halos mass function, the low-mass end is always higher than the high-mass end. Combining their results with our results of  $F'_{\text{sub}^A}$ , we see that the majority of the smallest survived sub-halos are not the descendants of the smallest sub-halos initially accreted, but rather, the descendants of those that are several times more massive. Fig. 8 plots  $M_{\text{acc}}$ , the mass at accretion, against the current mass,  $M_{\text{sub}}$  of sub-halos, in 200 host halos with  $M_h \approx 10^{13.6} h^{-1} M_\odot$ . Three different symbols denote different sub-halo accretion redshifts. It is clear that given  $M_{\text{sub}}$ , sub-halos accreted earlier generally have higher  $M_{\text{acc}}$ . At very low redshift ( $z \in [0, 0.05]$ ), sub-halos with a wide range of mass ( $\log_{10}[M_{\text{acc}}/M_h] \in [-3.3, -0.5]$ ) have been accreted by the main progenitor, and they have barely suffered from the mass loss so that  $M_{\text{sub}} \approx M_{\text{acc}}$ . However, for sub-halos that were accreted at high redshift

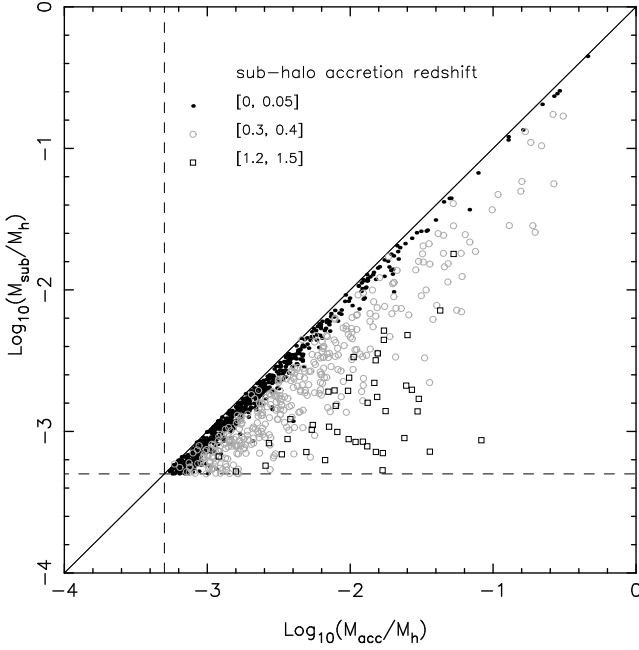


**Figure 8.**  $M_{\text{acc}}$  against  $M_{\text{sub}}$  for host halos of a given mass  $M_h$ . Points are from 200 randomly selected host halos with  $M_h \approx 10^{13.6} h^{-1} M_\odot$ . Different symbols denote different redshift intervals during which the sub-halos enter the main progenitor of the host halo. Dashed lines indicate the mass limitation in our analysis,  $M_{\text{lim}}$ .

( $z \in [1.2, 1.5]$ ), their  $M_{\text{acc}}$  are in general several times higher than  $M_{\text{sub}}$ .

Besides  $F'_{\text{subA}}$ , we also construct the “unevolved” mass function for the sub<sup>B</sup>-halo population,  $F'_{\text{subB}}$ , in the same way as  $F'_{\text{subA}}$ . Fig. 9 shows the ratio of  $F'_{\text{subB}}$  to  $F'_{\text{subA}}$ , for host halos with the same masses as in Fig. 7. We would like to remind the reader, once again, that the sub-halo mass used here is measured at the time when they were last found as isolated halos. Given a sub-halo mass, the vertical axis in Fig. 9 is the ratio of the number of survived sub-halos initially accreted by sub-branches to the number of survived sub-halos initially accreted by the main branch. In general,  $F'_{\text{subB}}/F'_{\text{subA}}$  is higher for massive host halos. For a given host halo mass, though, this ratio is always low ( $\sim 0.05$ ) at the high-mass end ( $\log_{10}[M_{\text{acc}}/M_h] > -0.7$ ), because mergers involving sub-halos with mass comparable to that of the final host halo can only happen on the main progenitor at very late time. There also appears to be a generally increasing trend in this ratio as sub-halo mass decreases down to a certain point. This may be due to two reasons. First, some small sub-halos that merge to sub-branches of the merging tree may survive if the time scale for disruption is long. Second, as the redshift increases, the number of mergers that happen on sub-branches is not negligible. The increasing trend changes its sign when sub-halo mass becomes very small. The reason is that small sub-halos that are able to survive were most likely accreted in the recent past, when main branch already dominates the merger incidences.

We can estimate the number fraction of sub<sup>B</sup>-halos among the whole survived sub-halo population, based on Fig. 9. This fraction is 9%, 17% and 28%, for host halo with

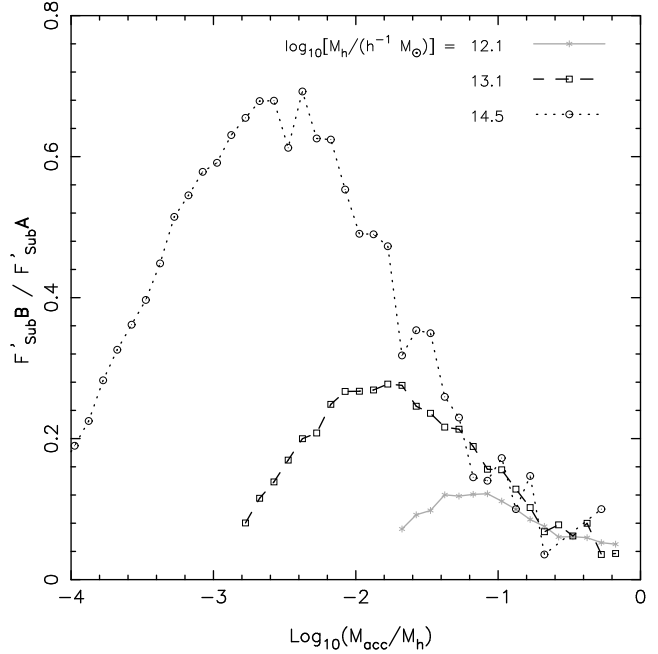


**Figure 9.** The ratio of  $F'_{\text{subB}}$  to  $F'_{\text{subA}}$  (see text for details). Different symbols indicate different host halo mass.

$M_h = 10^{12.1}, 10^{13.1}$ , and  $10^{14.5} h^{-1} M_\odot$ , respectively. Clearly, a significant fraction of sub-structures were sub-subhalos.

## 4 ACCRETION TIME OF SUB-HALOS

Although the USMFs give a quantitative description on the abundance of accreted sub-halos in the halo assembly history, it does not include the time (redshift) when the accretion happens. In galaxy formation models, the epoch when central galaxies became satellites is crucial as the physical processes relevant to galaxy evolution after the merger are expected to be different. It is therefore important to incorporate the sub-halo abundance at different redshift into our analysis.

### 4.1 Sub-halo mass function at given accretion time

#### 4.1.1 Main branch sub-halos and all sub-halos

We define the mass function of sub-halos at given accretion time (redshift) as follows,

$$f(z) = \frac{dF}{dz} = \frac{dN(z)}{d \ln(M_{\text{acc}}/M_h) dz}, \quad (4)$$

where  $F$  is the USMF,  $M_{\text{acc}}$  and  $M_h$  stand for the mass of sub-halos at the time of accretion and the mass of final host halo, respectively. To obtain  $f(z)$ , we choose a redshift interval  $\Delta z$  around a given  $z$ , and only count the number,  $N(z)$ , of sub-halos accreted during  $\Delta z$ . Within the redshift range of interest, we found  $\Delta z \sim 0.1$  effectively eliminates the noise and result in a relatively smooth shape of  $f$ .

Fig. 10 shows  $f$  of main branch sub-halos and all sub-halos for host halos with  $M_h = 10^{13.6} h^{-1} M_\odot$ . Interestingly,

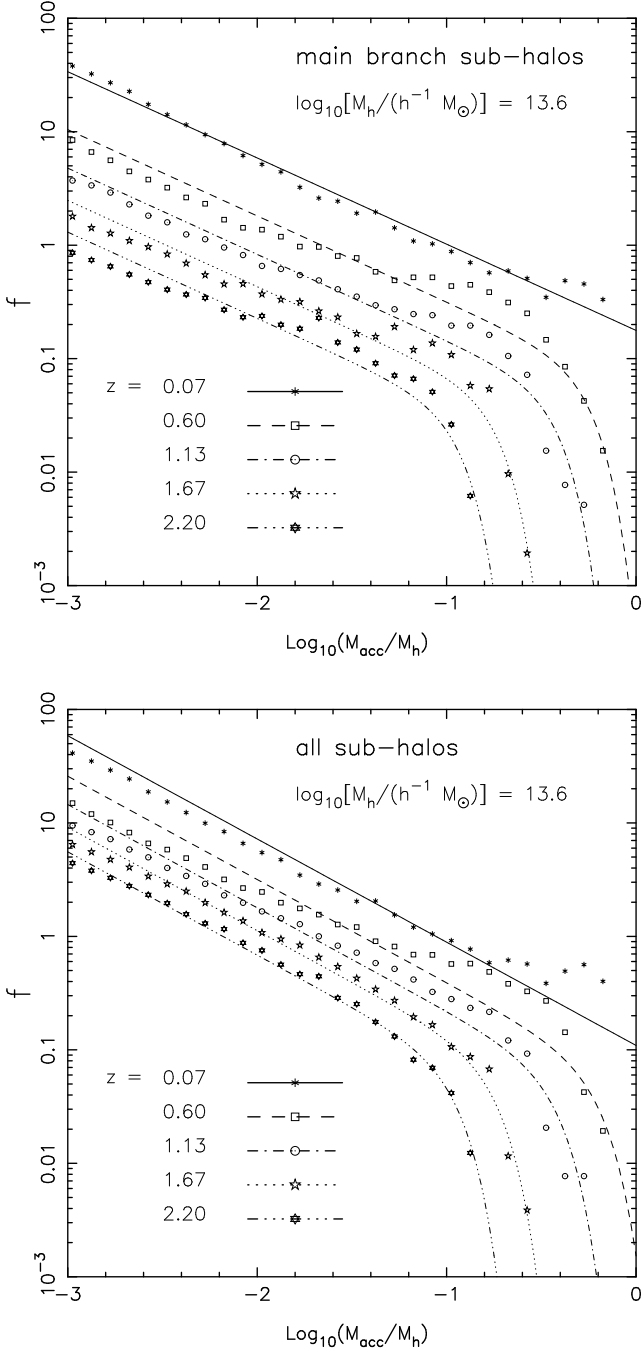


**Figure 10.** The mass function at accretion,  $f$ , of main branch (upper panel) and all (lower panel) sub-halos, given accretion redshift  $z$  and host halo mass  $10^{13.6} h^{-1} M_\odot$ . Different symbols and lines represent the data points and their best fits according to equation (1) (with fixed  $b$  and  $d$ , see text for details), at different redshifts.

in each case,  $f$  can still be described by equation (1) reasonably well. In addition, we found that the low-mass end power-index  $b$  of  $f$  are virtually independent of  $z$ , and is quite similar to the power-index we have obtained from the corresponding USMF. Since  $F = \int f dz$ , it is expected that the integration of  $f$  over  $z$  reproduces the low-mass end

power-index of  $F$ . The exponential shape of  $f$  (described by  $d$ ) at the high mass end also shows no obvious dependence on  $z$ . On the other hand, the amplitude of  $f$  and the transitional point where  $f$  deviates from the power-law clearly depend on the redshift. By keeping  $b$  and  $d$  fixed at the values obtained from the USMFs ( $b = -0.76$ ,  $d = 3.2$  for main branch sub-halos, and  $b = -0.91$ ,  $d = 3.0$  for all sub-halos), we fit  $f$  according to equation (1). Styled lines in Fig. 10 are the best-fits of  $f$  so obtained at the corresponding redshift.

In Fig. 11, we show the best-fit  $a$  and  $c$  against the redshift  $z$ , for host halo with different masses. Panels on the left are best-fit  $a$  and  $c$  for main branch sub-halos, while panels on the right are best-fit  $a$  and  $c$  for all sub-halos. In general,  $a$  always decreases monotonically as  $z$  increases, which implies that more sub-halos are accreted at lower redshift, especially for massive halos. Meanwhile,  $c$  shows positive correlation with  $z$ , which means that, compared with small sub-halos, the number of massive sub-halos drops more quickly as redshift increases. This disagrees with the result of Giocoli et al. (2008a). Their Fig. 1 shows that the USMF of the main branch sub-halos accreted before the halo formation time  $z_f$  is identical to the USMF of the sub-halos accreted after  $z_f$ , with proper adjustment in the amplitude  $a$  only. However, as we just mentioned, the number of massive sub-halos drops more quickly at higher redshift, and therefore simply offsetting the USMF of high-redshift sub-halos along the vertical direction cannot reconcile the lack of massive sub-halos and reproduce the shape at high-mass end of the USMF. Our results suggest that the relative abundance of massive sub-halos becomes higher at low redshift, consistent with the hierarchical formation of dark halos in a CDM model.

#### 4.1.2 Survived sub-halos accreted by the main progenitor

Given the time of merging, let us look at the mass function of sub-halos that survive as sub-structures in the final halo. We focus on sub<sup>A</sup>-halos, as the results for sub<sup>B</sup>-halos are similar. Based on the sub<sup>A</sup>-halo catalogue, we can register the time when they first became satellites of the main progenitor. We use  $f'_{\text{sub}^A}(z)$  to indicate the same sub<sup>A</sup>-halo mass function at given accretion time defined in equation (4).

Fig. 12 shows  $f'_{\text{sub}^A}$  at different redshifts, for host halo mass  $M_h = 10^{13.6} h^{-1} M_\odot$ . Note that the redshifts we used to plot  $f'_{\text{sub}^A}(z)$  is, on average, lower than the redshifts used in Fig. 10, because at higher redshift such as  $z > 1$ ,  $f'_{\text{sub}^A}$  becomes extremely small. Comparing Fig. 12 with the *upper panel* of Fig. 10, one can find both similarity and difference. At very low redshift ( $z = 0.07$ ),  $f'_{\text{sub}^A}$  and  $f$  are similar, due to the fact that sub-halos accreted by the main progenitor recently have a high survival rate. However, at higher redshift ( $z = 0.6$ ),  $f'_{\text{sub}^A}$  becomes much lower than  $f$ , owing to the dynamical effects that can effectively destroy the sub-halos accreted at early time.

As we have shown in Fig. 7, the “unevolved” mass function of sub<sup>A</sup>-halos,  $F'_{\text{sub}^A}$ , is not universal. Besides, the overall amplitude of  $F'_{\text{sub}^A}$ , also deviates substantially from the original USMF of main branch sub-halos,  $F_{\text{MB}}$ , especially at the low-mass end. The reason is clearly demonstrated in Fig. 12. When redshift increases,  $f'_{\text{sub}^A}$  becomes increasingly lower, especially for small sub-halos. Since  $F'$  is the integra-



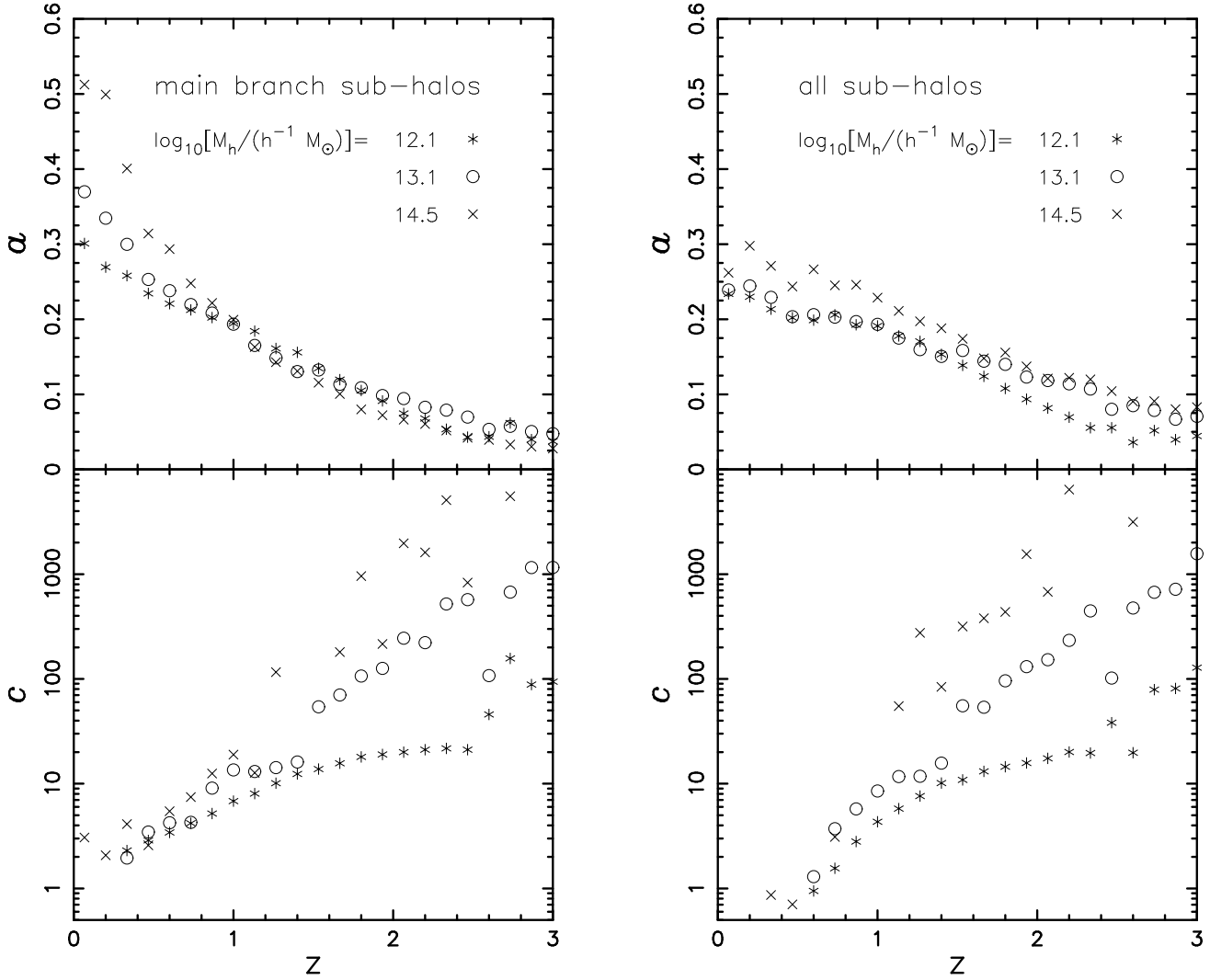


**Figure 11.** Best fit parameters  $a$  and  $c$ , given fixed  $b$  and  $d$ , of  $f$ , against redshift  $z$ . Panels on the left shows the result for main branch sub-halos, panels on the right shows the result for all sub-halos. Different symbols represent different host halo masses, as indicated in the figure.

tion of  $f'$  over  $z$ , it is therefore expected that  $F'_{\text{subA}}$  would have the behavior shown in Fig. 7.

#### 4.2 Distribution of sub-halo accretion time

In the previous sub-section, we have discussed the sub-halo mass function at accretion for given redshift. It clearly shows that the abundance of sub-halo accretion varies with redshift. In general, more sub-halos were accreted at lower redshift. It also seems that sub-halos with different masses may be accreted at different time.

Given sub-halo mass fraction  $M_{\text{acc}}/M_h$  and host halo mass  $M_h$ , Fig. 13 shows the number of sub-halo at the time of accretion as a function of redshift. Clearly, for fixed  $M_{\text{acc}}/M_h$ , small systems start to accrete sub-halo earlier. For instance, dark halos with  $10^{12.1} h^{-1} M_\odot$  begin to acquire sub-halos with  $M_{\text{acc}} = 0.03 M_h$  at  $z = 5 \sim 6$ , while for halos with  $10^{14.5} h^{-1} M_\odot$ , this happens at  $z \sim 3$ . Compared with small sub-halos, large sub-halos enter the system fairly late.

Nearly all sub-halos with mass  $M_{\text{acc}} = 0.3 M_h$  enter their host at redshift  $z < 1.5$ .

For fixed host halo mass, large fraction of small sub-halos enter the system through sub-branches, especially at high redshift such as  $z > 1$ , while massive sub-halos (i.e.,  $M_{\text{acc}}/M_h = 0.3$ ) enter the systems only through the main branch, at relatively lower redshift. In addition, as discussed in Section 3, almost all survived sub-halos (sub<sup>A,B</sup>-halos) were accreted at redshift  $z < 1$ , and more sub<sup>A,B</sup>-halos are likely to survive in massive systems.

On average, sub-halo accretion of dark halos is determined by the initial CDM density power-spectrum and shows hierarchical signature. The sub-halo accretion for individual dark halos, however, can be very stochastic. Let  $P_{1/2, M_{\text{acc}}/M_h}(z)$  denotes the probability distribution function (PDF) of the redshift  $z$  by which the host halo has acquired 1/2 of the total number of the *main branch* sub-halos with fixed mass  $M_{\text{acc}}/M_h$ . Fig. 14 shows  $P_{1/2, M_{\text{acc}}/M_h}$  as a function of  $z$ , for sub-halos with mass  $M_{\text{acc}} = (2 - 5)\% M_h$ .

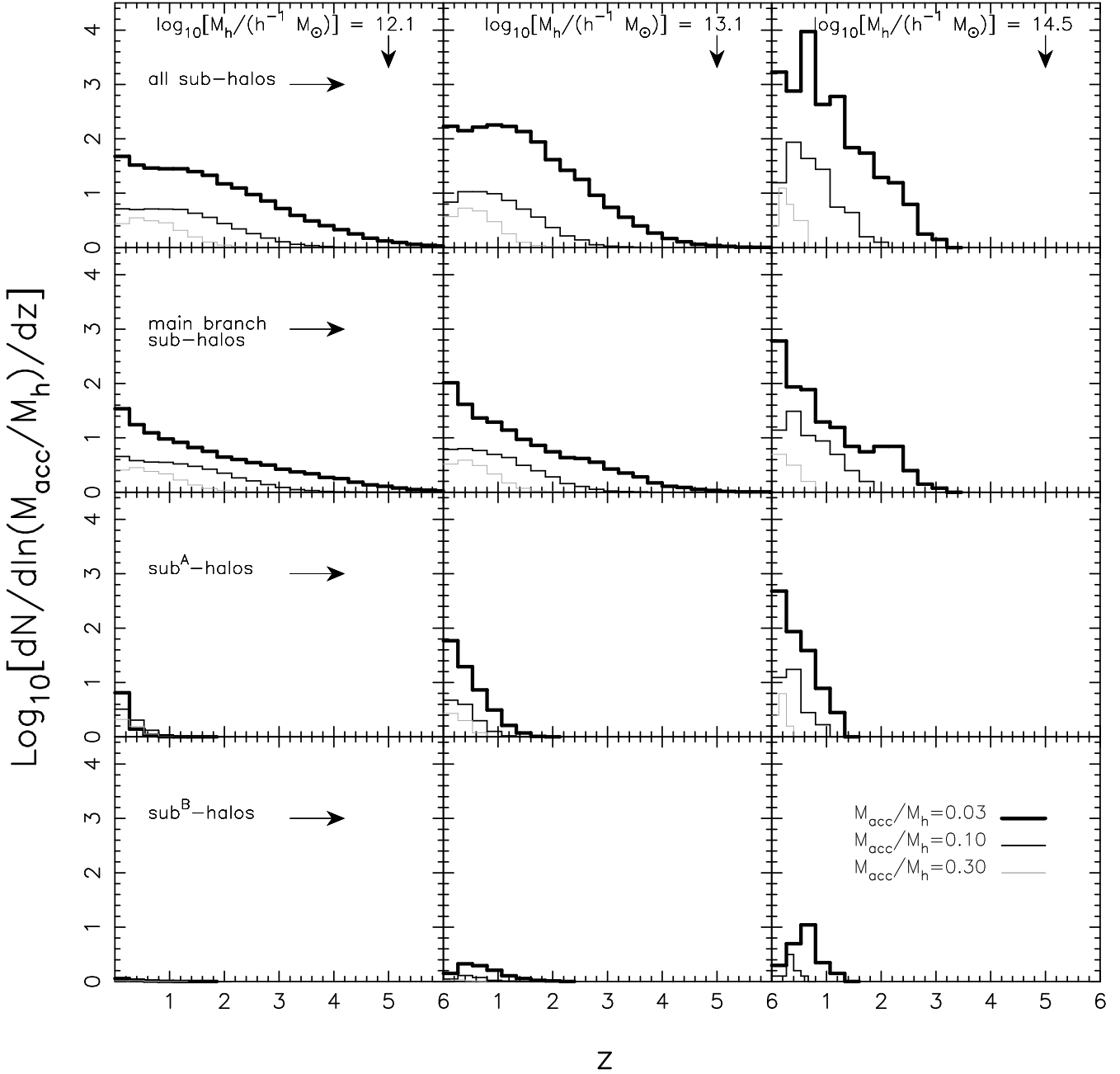


**Figure 13.** Sub-halo mass function at the time of accretion against redshift  $z$ , given sub-halos mass  $M_{\text{acc}}$  and final host halo mass  $M_h$ . Each row represents one definition of sub-halo, and different columns represent different host halo masses, as indicated by the arrows. There are three lines in every panel. Thick solid line is for sub-halo with  $M_{\text{acc}} = 0.03M_h$ , light solid line is for sub-halo with  $M_{\text{acc}} = 0.1M_h$  and gray solid line is for sub-halo with  $M_{\text{acc}} = 0.3M_h$ .

We choose  $M_{\text{acc}} \sim 3\%$  of  $M_h$  to ensure that the majority ( $> 75\%$ ) of our catalogued halos would have more than one sub-halo mergers with such sub-halo mass. Clearly, the redshift covers a wide range:  $z \in (0, 6), (0, 5), (0, 3)$  for halos with  $M_h = 10^{12.1}, 10^{13.1},$  and  $10^{14.5} h^{-1} M_\odot$ , respectively. This indicates that, even for the same sub-halo mass and host halo mass, sub-halo merger is a highly stochastic process.

## 5 SUMMARY

Halo-halo merger is the basis of galaxy merger. The time of merger and the sub-halo mass at the time of merger are two important halo properties relevant for modeling galaxy formation. In this paper, we study the mass function and other properties of sub-halo mergers during the dark halo assembly history. We studied three kinds of sub-halos: main branch sub-halos, all sub-halos, and sub-halos that survived the dynamical disruption after merger. We also studied the redshift dependence and evolution of sub-halo mass func-

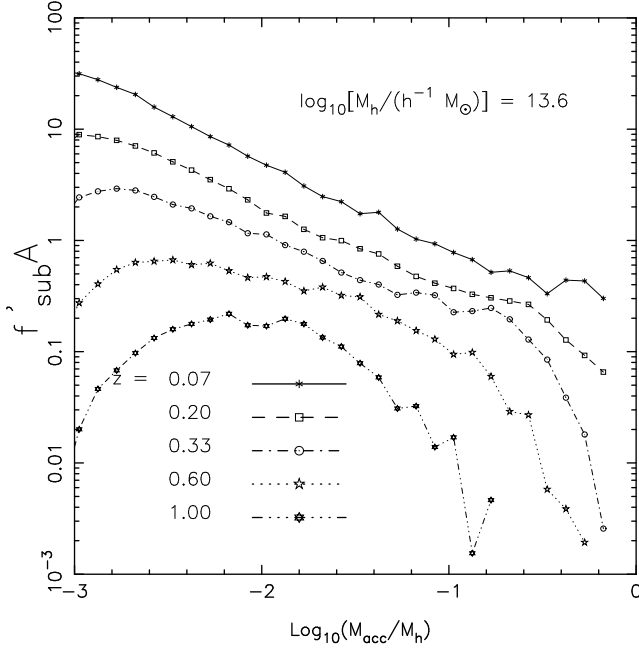


**Figure 12.** The sub<sup>A</sup>-halo mass function at accretion,  $f'_{\text{sub}A}$ , given accretion redshift  $z$  and host halo mass  $M_h = 10^{13.6} h^{-1} M_\odot$ . Different symbols connected with styled lines represent results at different redshifts.

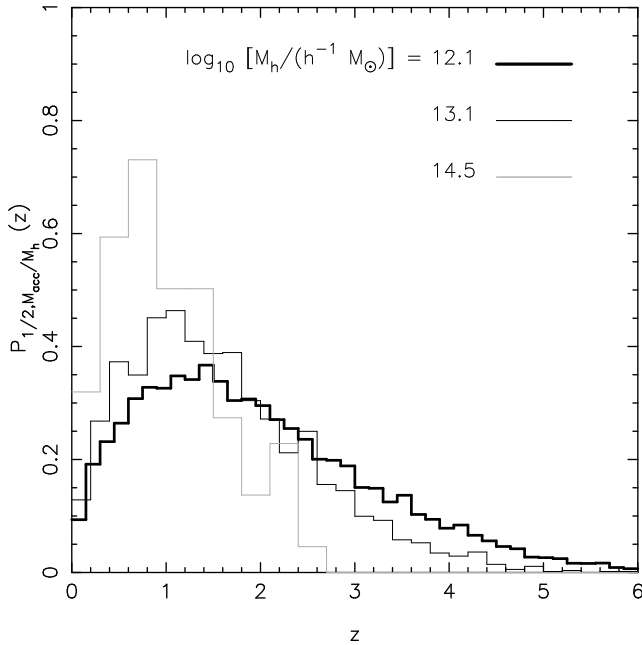


**Figure 14.**  $P_{1/2, M_{\text{acc}}/M_h}(z)$ , given main branch sub-halo mass  $M_{\text{acc}} = (2 - 5)\% M_h$ . Different lines represent different host halo masses.

tion, as well as the distribution of the redshift at which a sub-halo is accreted. Our main findings can be summarized as follows:

(i) We confirmed the previous result that the average unevolved mass function of main branch sub-halos follows a universal functional form, regardless of host halo

mass (Giocoli et al. 2008a). In addition, we found that this function is also independent of the redshift of the host halo.

(ii) The unevolved mass function of all sub-halos that have been accreted during the entire halo assembly history is also a universal function that shows no host-halo-mass or redshift dependence.

(iii) There are roughly the same or double number of sub-halos, with mass 1% or 0.1% of the final host halo mass, that were accreted by progenitors other than the main progenitor. The amount is significant considering the central galaxies that merge along with such sub-halos may be more resistant to dynamical disruption that destroy the sub-halos.

(iv) The mass function of survived sub-halos at the time of merging is not universal, due to the fact that large fraction of sub-halos that merged at early time are destroyed by dynamical friction and tidal stripping. The fraction of sub-subhalos can account for up to 30% of the whole survived sub-halo catalogue in cluster-sized dark halos, and decreases with host halo mass.

(v) In general, more sub-halos are accreted at lower redshift. However, for given host halo and sub-halo mass, the accretion time has very broad distribution. Survived sub-halos are accreted late and therefore represent a very special subset of the total sub-halo population accreted into host halos.

## ACKNOWLEDGMENTS

The *Millennium Simulation* was carried out as part of the programme of the Virgo Consortium on the Regatta supercomputer of the Computing Centre of the Max-Planck Society in Garching. YL would like to thank Liang Gao for the help on the simulation data. HJM would like to acknowledge the support of NSF AST-0607535, NASA AISR-126270 and NSF IIS-0611948.

## REFERENCES

- Angulo R. E., Lacey C. G., Baugh C. M., Frenk C. S., 2008, preprint (astro-ph/0810.2177)
- Barnes J., Efstathiou G., 1987, ApJ, 319, 575
- Barnes J., Hernquist L., 1996, ApJ, 471, 115
- Berlind A. A., Weinberg D. H., 2002, ApJ, 575, 587
- Bond J. R., Cole S., Efstathiou G., Kaiser N., 1991, ApJ, 379, 440
- Bullock J. S., Dekel A., Kolatt T. S., Kravtsov A. V., Klypin A. A., Porciani C., Primack J. R., 2001a, ApJ, 555, 240
- Bullock J. S., Kolatt T. S., Sigad Y., Somerville R. S., Kravtsov A. V., Klypin A. A., Primack J. R., Dekel A., 2001b, MNRAS, 321, 559
- Cole S., Lacey C., 1996, MNRAS, 281, 716
- De Lucia G., Blaizot J., 2007, MNRAS, 375, 2
- De Lucia G., Kauffmann G., Springel V., White, S. D. M., Lanzoni B., Stoehr F., Tormen G., Yoshida N., 2004, MNRAS, 348, 333
- Fakhouri O., Ma C. P., 2008, MNRAS, 386, 577
- Gao L., White S. D. M., Jenkins A., Stoehr F., Springel V., 2004, MNRAS, 355, 819

- Gao L., Springel V., White S. D. M., 2005, MNRAS, 363, 66
- Giocoli C., Torman G., van den Bosch F. C., 2008a, MNRAS, 386, 2135
- Giocoli C., Pieri L., Tormen G., MNRAS, 2008b, 387, 689
- Hopkins P. F., Hernquist L., Cox T. J., Di Matteo T., Robertson B., Springel V., 2006, ApJS, 163, 1
- Kim J., Park C., Choi Y., 2008, ApJ, 683, 123
- Lacey C., Cole S., 1993, MNRAS, 262, 627
- Lemson G., Kauffmann G., 1999, MNRAS, 302, 111
- Li Y., Mo H. J., van den Bosch F. C., Lin W. P., 2007, MNRAS, 379, 689
- Li Y., Mo H. J., Gao L., 2008, MNRAS, 389, 1419
- Lu Y., Mo H. J., Katz N., Weinberg M. D., 2006, MNRAS, 368, 1931
- Maller A. H., Katz N., Keres D., Dave R., Weinberg D. H., 2006, ApJ, 647, 763
- Mandelbaum R., Seljak U., Kauffmann G., Hirata C. M., Brinkmann J., 2006, MNRAS, 368, 715
- McIntosh D. H., Guo Y., Hertzberg J., Katz N., Mo H. J., van den Bosch F. C., Yang X., 2008, MNRAS, 388, 1537
- Mo H. J., White S. D. M., 1996, MNRAS, 282, 347
- Naab T., Burkert A., 2003, ApJ, 597, 893
- Navarro J. F., Frenk C. S., White S. D. M., 1997, ApJ, 490, 493
- Sheth R. K., 2003, MNRAS, 345, 1200
- Sheth R. K., Mo H. J., Tormen G., 2001, MNRAS, 323, 1
- Sheth R. K., Tormen G., 1999, MNRAS, 308, 119
- Springel V. et al., 2005, Nat., 435, 639
- Springel V., White S. D. M., Tormen G., Kauffmann G., 2001, MNRAS, 328, 726
- Tinker J. L., Weinberg D. H., Zheng Z., Zehavi I., ApJ, 2005, 631, 41
- van den Bosch F. C., Tormen G., Ciocoli C., 2005, MNRAS, 359, 1029
- van den Bosch et al., 2007, MNRAS, 376, 841
- Wang L., Li C., Kauffmann G., De Lucia G., 2006, MNRAS, 371, 537
- Wechsler R. H., Bullock J. S., Primack J. R., Kravtsov A. V., Dekel A., 2002, ApJ, 568, 52
- Wetzel A. R., Cohn J. D., White M., 2008, preprint (astro-ph/0810.2537)
- Yang X. H., Mo H. J., van den Bosch F. C., 2003, MNRAS, 339, 1057
- Yang X. H., Mo H. J., van den Bosch F. C., 2009, ApJ, 693, 830
- Zhao D. H., Mo H. J., Jing Y. P., Börner G., 2003, MNRAS, 339, 12
- Zheng Z. et al., 2005, ApJ, 633, 791